A numerical study of quantum decoherence

Riccardo ADAMI[1] and Claudia NEGULESCU[2]

1 Dipartimento di Matematica e Applicazioni, Università di Milano Bicocca
via R. Cozzi, 53 20125 Milano, Italy

2 CMI/LATP (UMR 6632), Université de Provence
39, rue Joliot Curie, 13453 Marseille Cedex 13, France

e-mail : riccardo.adami@unimib.it ; claudia.negulescu@cmi.univ-mrs.fr

February 23, 2011

Abstract

The present paper provides a numerical investigation of the decoherence effect induced on a quantum heavy particle by the scattering with a light one. The time dependent two-particle Schrödinger equation is solved by means of a time-splitting method. The damping undergone by the non-diagonal terms of the heavy particle density matrix is estimated numerically, as well as the error in the Joos-Zeh approximation formula.

Keywords : Quantum mechanics, Schrödinger equation, Heavy-light particle scattering, Interference, Decoherence, Numerical discretization, Numerical analysis, Splitting scheme.

1 Introduction

Quantum decoherence is nowadays considered as the key concept in the description of the transition from the quantum to the classical world (see e.g. [6, 7, 9, 19, 20, 22, 24]).

As it is well-known, the axioms of quantum mechanics allow superposition states, namely, normalized sums of admissible wave functions are once more admissible wave functions. It is then possible to construct non-localized states that lack a classical interpretation, for instance, by summing two states localized far apart from each other. The observable mark of such a quantum mechanical superposition state is the presence of interference fringes in the probability distribution associated to the state (see e.g. [11]). We stress that this phenomenon does not have a classical explanation: classically, a probability distribution evolving freely in the phase space of a single particle follows the free Liouville equation, so, by linearity, two colliding probability densities sum up without creating an interference pattern.

Nonetheless, at human scale no interference is revealed, so the question arises, on how does the interference pattern disappear. Such a phenomenon is called *decoherence* and its explanation lies in the fact that macroscopic objects undergo a continuous interaction with an external environment (such as air molecules, fields), which causes the loss of the phase relations between the different states in the superposition. Thus, the state of the system becomes a statistical mixture in which the quantum effects are suppressed.

In this sense, the system loses its quantum nature and then its state admits a classical interpretation.

Understanding decoherence is important not only in the foundations of quantum mechanics, but also in applied physics. For example, in quantum computation (QC), electron spin resonance (ESR), and nuclear magnetic resonance (NMR) it is of paramount importance to preserve the quantum behaviour, so decoherence is not desired and efforts are made in order to avoid it [27,29]. On the other hand, in quantum interference effect transistors (QuIET) decoherence is exploited to control the quantum current flow [28]. In such devices, decoherence acts like a switch to modulate the current flow, the device being switched "off" in the completely coherent state and "on" when interference disappears.

We remark that the transition from the quantum to the classical regime due to decoherence is different from the semi-classical limit, where the classical behaviour is recovered exploiting the smallness of Planck's constant. Let us stress three main differences to this regard: first, decoherence requires an open system, i.e. a system that interacts with an environment; second, decoherence acts at the length-scale of the interference pattern, whereas a typical semi-classical procedure consists in evaluating a macroscopic observable on a fast oscillating probability distribution; third, decoherence is a dynamical effect: it grows with time, whereas the semi-classical limit can be performed in the stationary framework too. Furthermore, at least qualitatively, $\hbar$ plays no role in the mechanism of decoherence: nevertheless, from a quantitative point of view, in many models of physical relevance the time-scale of the decoherence owes its shortness to the smallness of $\hbar$ (see e.g. [24]). Even though in this paper $\hbar$ acts as a constant, we keep writing it explicitly in formulas, in view of possible future investigation on a more precise determination of the decoherence rate.
In spite of its recognized relevance, there are still few rigorous results on decoherence, both from the analytical ([1–3, 8, 10, 12, 14, 15]) and the numerical ([5]) point of view.

The aim of this paper is to investigate numerically the mechanism of decoherence on the simplest model in which it takes place, namely a heavy particle that scatters a light one. Therefore, the system we monitor is a quantum particle and the environment is another quantum particle, considerably lighter than the first one. The two particles interact with each other via a repulsive potential and, due to the low mass-ratio, the light particle is scattered away while the heavy particle remains almost unperturbed. It turns out that, at leading order in the mass ratio, the only effect of the interaction on the heavy particle is the destruction of the interference pattern.

We would like to point out here that, even though the small mass ratio had already been employed in the well-known Born-Oppenheimer approximation ([18]), a different physical situation is described in the present study, as no bound states are present and the interaction between the particles can be described as an instantaneous scattering process.

The analytical study of the one dimensional, two-body problem in the small mass ratio and with a zero-range potential was performed in [14]. In [2] the analysis was extended to the three-dimensional case in the presence of a fairly general interaction,

and in [3] a model with an arbitrary number of heavy particles interacting with an arbitrary number of light ones was investigated.

The present paper provides a numerical resolution of the 2D time-dependent Schrödinger equation. As a further step, such a resolution is exploited in order to describe the dynamics of the two-particle system in the hypothesis of small mass ratio.

In order to summarize our results, we need to be more specific and to anticipate the content of Section 2. Consider the case of a particle of mass M, initially lying in the quantum superposition of two localized and separated "bumps", i.e. described by a wave function like

$$\phi_0(X) := \varphi_0(X - X_0)\, e^{\frac{-\mathbf{i}P_H X}{\hbar}} + \varphi_0(X + X_0)\, e^{\frac{\mathbf{i}P_H X}{\hbar}},$$

where $P_H > 0$, $X_0 > 0$. The function φ_0 can be thought of as a Gaussian (as we shall do in (2.6)). The two bumps are moving against each other.
If the particle does not interact with the external environment, then at time $\bar{t} = MX_0/P_H$ (corresponding to the time when the two bumps completely overlap) the probability of finding the particle at a position X reads

$$\rho_H^{\text{free}}(\bar{t}, X) = 2\left(1 + cos\left(2\frac{P_H}{\hbar}X\right)\right)\left|\left[\mathcal{U}^M(\bar{t})\varphi_0\right](X)\right|^2, \tag{1.1}$$

where $\mathcal{U}^M$ represents the free Schrödinger evolution for the heavy particle (the precise definition will be given in (2.9)). The presence of opposite phases in the two components yields an oscillating term that describes an interference pattern composed of alternating fringes of high and low probability density, embodied in the term $cos\left(2\frac{P_H}{\hbar}X\right)$.

On the other hand, according to a widely accepted heuristics, if the same particle interacts with another particle of smaller mass, then the dynamics becomes more complicated and the quantity given in (1.1) can be replaced (in a suitable approximation) by

$$\rho_H^{\text{interacting}}(\bar{t}, X) = 2\left(1 + \Lambda\, cos\left(2\frac{P_H}{\hbar}X\right)\right)\left|\left[\mathcal{U}^M(\bar{t})\varphi_0\right](X)\right|^2, \tag{1.2}$$

where the presence of a constant factor $0 < \Lambda < 1$ shows that the interference fringes are damped. We stress that Λ depends on the chosen interaction potential and on all parameters in the model and in the initial data. The rigorous results in [2, 3, 14] show that formula (1.2) is a correct approximation up to an error

$$\text{Error} \leq C(\sqrt{\varepsilon} + \sigma_H),$$

where the small parameter ε is the ratio between the mass of the light particle and the mass of the heavy one and σ_H is the width of the bumps in the initial state of the heavy particle (see eq. (2.6)).

We stress that the small mass ratio hypothesis is the key assumption in order to get a density distribution like in (1.2), in which *decoherence is the only physical effect*. This means that, due to such a hypothesis, one can completely neglect energy exchange between the two particles and other effects of deformation and of repulsion of the wave packets. In other words, dissipative phenomena occur on a longer time scale, typical of decoherence of Brownian particles (see e.g. [7]).

Our numerical results complete the cited theoretical analysis, in the sense that we explicitly evaluate the decoherence coefficient Λ, analyze its dependence on the strength of the interaction, and estimate the constant C in the error, up to now only implicitly known.
To this aim, we extract numerically a regime in which decoherence is the dominating effect, while dissipation can be neglected. Furthermore, we show that, at least with our choice of a potential, this purely decoherent regime is already reached when the mass ratio is of the order of 10^{-3}. The result in [3], although rigorous, does not permit such evaluation due to the presence of an unknown constant in the error estimate.

Our results can be summed up as follows: first, we show that, at least for our model, the Joos-Zeh approximation is effective for values of the mass ratio of the order of 10^{-3} (small, but not extremely small), which is the order of magnitude of the mass ratio of nucleons and electrons. Second, we found that such approximation is no longer valid as the interaction becomes too strong. Third, we found that, as the strength of the interaction increases the most important effect beyond decoherence lies in the repulsion of the two bumps: quite surprisingly, we hardly see a deformation of the probability profile in our experiments.

The strongest limitation of our results is that, at this stage, they correspond only to a particular two-body model. A further step shall be to extract the physical relevant parameters from the interaction potential and to extend the present results to a wider class of models.

In particular, the theoretical analysis can be extended to the case of an environment made of many light particles. In this case, the physics involved would remain basically unchanged, but the resulting coefficient Λ would increase with the number of light particles, and thus of interactions. Roughly speaking, in the presence of an environment made of N light particles lying initially in the same state and interacting with the heavy particle in the same fashion, a coefficient $\Lambda_N = \Lambda^N$ is expected to be found instead of Λ in (1.2) (see [3]).

However, with the present numerical model the possibility of considering several light particles is definitely out of reach. This is due to the fact that the wave function depends on the position variable of all particles, which leads to high dimensional systems as the number of particles significantly increases. In the forthcoming paper [4] a different and efficient model will be considered, permitting to treat multiple collisions with no additional numerical effort.

Anyway, the physics involved in this simple model is by no way different from the physics of a heavy particle in an environment of many light particles: the amount of decoherence yielded by many collisions is nothing but the resultant of the amount of decoherence produced by any single collision. So, any theoretical analysis of the so-called collisional decoherence must start from the analysis of a two-body problem and involves the study of a two-particle scattering (see e.g. [19], [21]).

The outline of this paper is the following. In Section 2 we state the mathematical problem and introduce the Joos-Zeh approximation for the two-body wave function, that holds in the small mass-ratio regime. Furthermore, we define the decoherence coefficient Λ. In Section 3 we present the numerical scheme employed for the resolution

of the 2D time-dependent Schrödinger equation and comment on the obtained numerical results. In particular, we investigate the behaviour of the decoherence coefficient Λ as a function of the strength of the interaction. In Section 4 we sketch, at a qualitative level, a different insight on decoherence, as suggested by the analysis of the dynamics in the classical two-particle configuration space. A detailed numerical analysis of the chosen numerical scheme will be given in the forthcoming paper [23] .

2 Model problem and mathematical study

2.1 The dynamics

We analyze the dynamics of a quantum system composed of a heavy and a light particle, interacting with each other. We consider the heavy particle as the "system", and monitor the decoherence induced on it by the light one, that plays the role of the "environment". According to the axioms of non-relativistic quantum mechanics, the evolution of the two-particle wave function $\psi(t, x, X)$ is driven by the time-dependent Schrödinger equation

$$\mathbf{i}\hbar\,\partial_t\psi(t,x,X) = -\frac{\hbar^2}{2M}\Delta_X\psi(t,x,X) - \frac{\hbar^2}{2m}\Delta_x\psi(t,x,X) + \alpha V(|x-X|)\,\psi(t,x,X)\,, \quad (2.3)$$

where t denotes the time variable, x is the spatial coordinate of the light particle, and X is the spatial coordinate of the heavy particle. The symbols M and m represent the masses of the heavy and the light particle, respectively, so $m \ll M$, and $\hbar$ is the reduced Planck's constant. The parameter $\alpha \in \mathbb{R}^+$ shall in the sequel modulate the strength of the particle interaction.

The potential V is chosen in Gaussian form, namely

$$V(r) := \frac{1}{\sqrt{2\pi}\,\sigma} e^{-\frac{r^2}{2\sigma^2}}\,, \quad \sigma \in \mathbb{R}^+ \quad \text{and} \quad r \in \mathbb{R}\,. \quad (2.4)$$

Notice that V is positive and regular; such a choice implies that we are analyzing a scattering regime, i.e. the interaction is repulsive and no bound states are present.

We assume that at the initial time $t = 0$ the wave function of the two-particle system reads

$$\psi(0,x,X) = \psi_0(x,X) = \left(\varphi_0(X - X_0)\, e^{\frac{-\mathbf{i}P_H X}{\hbar}} + \varphi_0(X + X_0)\, e^{\frac{\mathbf{i}P_H X}{\hbar}}\right)\chi_0(x)\,. \quad (2.5)$$

The initial condition (2.5) is taken in factorized form, i.e. at time zero the two particles are assumed to be uncorrelated. The two functions φ_0 and χ_0 are Gaussian wave packets

$$\varphi_0(X) := \frac{\beta}{(2\pi)^{1/4}\sqrt{\sigma_H}} e^{-\frac{X^2}{4\sigma_H^2}}\,, \quad \chi_0(x) := \frac{1}{(2\pi)^{1/4}\sqrt{\sigma_L}} e^{-\frac{(x-x_0)^2}{4\sigma_L^2}}\, e^{\frac{-\mathbf{i}P_L x}{\hbar}}\,, \quad (2.6)$$

with $\beta \in \mathbb{R}^+$ chosen so that the initial condition satisfies $\|\psi_0\|_{L^2(\mathbb{R}^2)} = 1$.

Let us remark that $-P_L/m$ is the group velocity of the light particle wave function, whereas $-P_H/M$ and P_H/M are the group velocities of the two wave packets that compose the state of the heavy particle.

2.2 Interference

As it is widely known, the physical interpretation of $\psi(t,x,X)$, known as the Born's rule, states that the quantity $|\psi(t,x,X)|^2 dxdX$ represents the probability to find at time t the light particle in the volume dx around the position x, and the heavy particle in the volume dX around X.

From the two-particle wave function $\psi(t,x,X)$ one can get the physically significant one-particle densities $\rho_L(t,x)$ and $\rho_H(t,X)$, related respectively to the light and to the heavy particle, by an integration on the degree of freedom of the other particle, namely

$$\rho_L(t,x) := \int_{-\infty}^{\infty} |\psi(t,x,X)|^2 \, dX \,, \quad \rho_H(t,X) := \int_{-\infty}^{\infty} |\psi(t,x,X)|^2 \, dx \,. \tag{2.7}$$

In Figure 1 we show the initial density function of the heavy particle, i.e. $\rho_H(0,X)$.

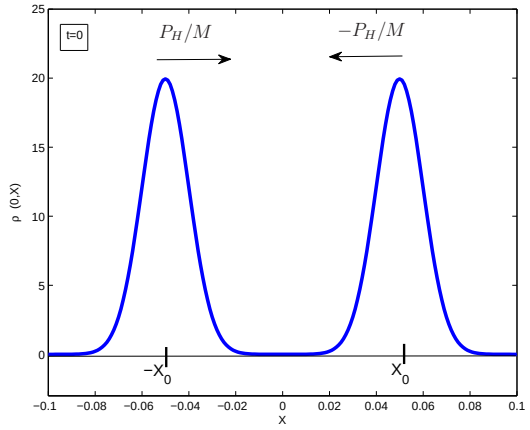

Figure 1: Initially, the heavy particle is given under the form of two wave-packets moving against each other. Here is plotted the corresponding probability density function.

If there is no interaction between the two particles (i.e. if $\alpha = 0$ in (2.3)), then the dynamics of the heavy particle is described by the free 1D Schrödinger equation

$$\begin{cases} \mathbf{i}\hbar\, \partial_t \varphi(t,X) = -\dfrac{\hbar^2}{2M} \Delta_X \varphi(t,X) \,, \quad (t,X) \in (0,T) \times \mathbb{R} \\ \varphi(t=0,X) = \varphi_0(X - X_0)\, e^{\frac{-\mathbf{i}P_H X}{\hbar}} + \varphi_0(X + X_0)\, e^{\frac{\mathbf{i}P_H X}{\hbar}} \end{cases},$$

whose solution reads

$$\begin{aligned} \varphi(t,X) \;\; = \;\; & e^{-i\frac{P_H^2 t}{2M\hbar}}\, e^{\frac{-iP_H X}{\hbar}}\, (\mathcal{U}^M(t)\varphi_0)(X - X_0 + P_H t/M) \\ & + e^{-i\frac{P_H^2 t}{2M\hbar}}\, e^{\frac{iP_H X}{\hbar}}\, (\mathcal{U}^M(t)\varphi_0)(X + X_0 - P_H t/M), \end{aligned} \tag{2.8}$$

where we introduced the unitary free Schrödinger group $\mathcal{U}^M(t)$, whose action is

$$(\mathcal{U}^M(t)\varphi_0)(X) = \sqrt{\frac{M}{2\pi i\hbar t}} \int_{-\infty}^{+\infty} e^{i\frac{M(X-X')^2}{2\hbar t}} \varphi_0(X')\, dX'. \tag{2.9}$$

Applying the Born's rule to (2.8) one finds the following evolution of the heavy particle density function

$$\rho_H(t,X) := \left|(\mathcal{U}^M(t)\varphi_0)(X - X_0 + P_H t/M)\right|^2 + \left|(\mathcal{U}^M(t)\varphi_0)(X + X_0 - P_H t/M)\right|^2 + 2\mathrm{Re}\left[e^{-2i\frac{P_H}{\hbar}X}(\mathcal{U}^M(t)\varphi_0)(X - X_0 + P_H t/M)\overline{(\mathcal{U}^M(t)\varphi_0)(X + X_0 - P_H t/M)}\right]. \tag{2.10}$$

At time $\overline{t} = \frac{X_0 M}{P_H}$, which corresponds to the complete overlap of the two heavy particle bumps, the probability density reads

$$\rho_H(\overline{t},X) = 2\left(1 + cos(2\frac{P_H}{\hbar}X)\right)\left|\left[\mathcal{U}^M(\overline{t})\varphi_0\right](X)\right|^2. \tag{2.11}$$

Let us stress that the last term in (2.10) as well as the term $cos(2\frac{P_H}{\hbar}X)$ in (2.11) describe the appearance of the interference pattern in the density function of the heavy particle, in the region where the two bumps overlap (see Figure 2 on the left). This is the fully quantum mechanical picture.

It is not immediate to understand which is the classical counterpart of (2.11). Indeed, it is well-known that no classical free evolution can reproduce the quantum evolution of the probability densities of both the position and the momentum for the heavy particle (see e.g. [17]). Nevertheless, there exists a classical distribution in the phase space that reproduces the quantum evolution of a single Gaussian bump. We interpret the sum of two such distributions as the classical counterpart of the quantum free evolution of our two-bump initial data. Since it evolves by the free Liouville equation, that is linear, no interference can arise and we can understand

$$\rho_{H,C}(t,X) := \left|(\mathcal{U}^M(t)\varphi_0)(X - X_0 + P_H t/M)\right|^2 + \left|(\mathcal{U}^M(t)\varphi_0)(X + X_0 - P_H t/M)\right|^2, \tag{2.12}$$

as the classical correspondent of (2.11). Eq. (2.12) implies $\rho_{H,C}(\overline{t},X) = 2\left|(\mathcal{U}^M(t)\varphi_0)(X)\right|^2$, as plotted in Figure 2, on the right.

We investigate numerically in this paper how the interaction with the light particle induces the decay of the last term in (2.10) and, consequently, how the interference pattern is lowered. This is the so-called "decoherence effect".

2.3 Decoherence according to Joos-Zeh

The physical mechanism at the origin of decoherence has been described in a famous paper by Joos and Zeh ([22]). In this paper, the environment is modeled as a gas of many light particles, and a repulsive force acts between the heavy particle and each light particle. The dynamics of such many-particle system is then depicted as a sequence of binary collisions.

Owing to the difference in the mass of the particles involved, in any such collision the state of the heavy particle remains basically unchanged while the light particle is scattered away. If the initial state of the heavy particle is the superposition of two localized "bumps", as in (2.5), then the light particle is scattered separately by both

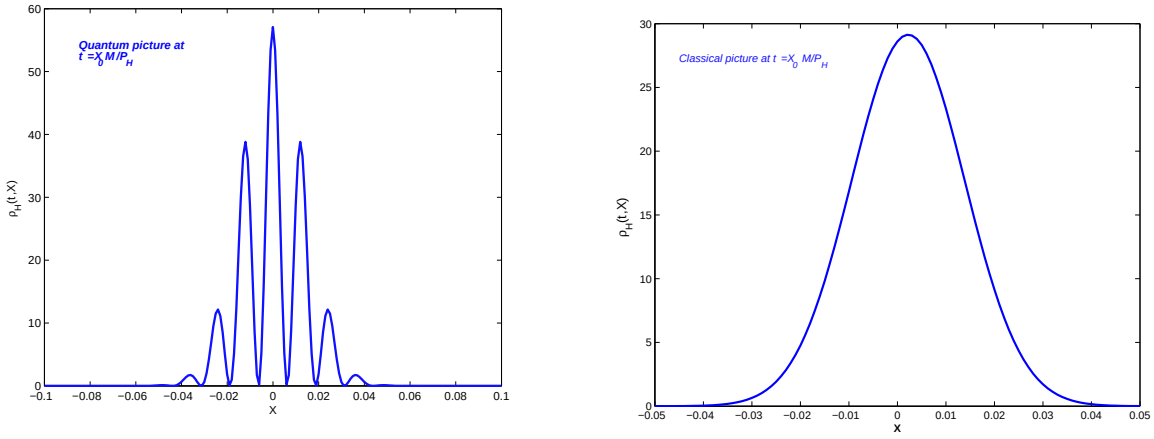

Figure 2: Left: Interference pattern: quantum superposition of the two bumps in the probability density of the heavy particle. Right: Classical superposition of the two bumps in the probability density of the heavy particle. Notice the difference in the scale of the vertical axes.

bumps, giving rise to two scattered waves. Moreover, as the two bumps are localized at different points, the respective scattered waves of the light particle cannot be equal. As a net effect of the presence of two different scattered wave functions of the light particle, associated each to the corresponding bump of the heavy particle, the collisions provide a sensible modification of the probability density of finding the heavy particle at a fixed point: in particular, the presence of the fringes becomes less evident, i.e. decoherence occurs.

Applying the Joos-Zeh hypothesis to our model translates into assuming that, at time $\overline{t} = \frac{X_0 M}{P_H}$, the probability density of the heavy particle reads

$$\rho_{H,JZ}(\overline{t}, X) = 2\left(1 + \Lambda\, cos(2\frac{P_H}{\hbar}X)\right)\left|\left[\mathcal{U}^M(\overline{t})\varphi_0\right](X)\right|^2 , \tag{2.13}$$

where Λ is the *decoherence coefficient* that measures the attenuation of the interference fringes. Indeed, by (2.13), it appears that for $\Lambda = 1$ the approximation coincides with the fully quantum case, while for $\Lambda = 0$ the purely classical case is recovered. The case $0 < \Lambda < 1$ corresponds to an intermediate situation, where interference is only partially suppressed.

The mathematical derivation of the approximation (2.13) was provided in [3]. Following the line of this paper, we introduce the "mass ratio" parameter $\varepsilon := \frac{m}{M} \ll 1$ and modify the problem defined in (2.3)-(2.6) rescaling the potential by the factor ε^{-1}. The rescaled Schrödinger equation writes now

$$\mathbf{i}\hbar\,\partial_t\psi^\varepsilon(t,x,X) = -\frac{\hbar^2}{2M}\Delta_X\psi^\varepsilon(t,x,X) - \frac{\hbar^2}{2M\varepsilon}\Delta_x\psi^\varepsilon(t,x,X) + \frac{\alpha}{\varepsilon}V(|x-X|)\,\psi^\varepsilon(t,x,X). \tag{2.14}$$

Theorem 1.1. in [3] establishes that, for fixed $T > 0$, the solution $\psi_\varepsilon(t,x,X)$ of (2.14),(2.4)-(2.6) can be approximated for all times $t \in [0,T]$ by

$$\begin{aligned}\psi_a^\varepsilon(t,x,X) &= \frac{M\sqrt{\varepsilon}}{2\pi i\hbar t}\left[\int_{-\infty}^{+\infty} e^{i\frac{M(X-X')^2}{2\hbar t}}\varphi_0(X'-X_0)e^{-i\frac{P_H X'}{\hbar}}\right.\\ &\qquad\qquad \times\int_{-\infty}^{+\infty} e^{i\frac{M\varepsilon(x-x')^2}{2\hbar t}}\Omega_+^{-1}(X')\chi_0(x')\,dx'\,dX'\\ &\quad+\int_{-\infty}^{+\infty} e^{i\frac{M(X-X')^2}{2\hbar t}}\varphi_0(X'+X_0)e^{i\frac{P_H X'}{\hbar}}\\ &\qquad\qquad \left.\times\int_{-\infty}^{+\infty} e^{i\frac{M\varepsilon(x-x')^2}{2\hbar t}}\Omega_+^{-1}(X')\chi_0(x')\,dx'\,dX'\right], \qquad (2.15)\end{aligned}$$

and the error can be estimated as follows

$$\|\psi^\varepsilon(t)-\psi_a^\varepsilon(t)\|_{L^2(\mathbb{R}^2)} \le C_T\sqrt{\varepsilon}\,, \quad \forall t\in[0,T]\,, \qquad (2.16)$$

where the constant $C_T > 0$ depends on T, on the initial data (2.5) and on a suitable norm of the interaction potential αV.

In (2.15) the symbol $\Omega_+(X')$ denotes the Møller wave operator for the interaction given by a potential V centered at the point X', defined by (for more details see [26])

$$\Omega_+(X')\,\psi := \lim_{\varepsilon\to 0} e^{\frac{it}{\varepsilon}\left[-\frac{\hbar}{2M}\partial_x^2+\frac{\alpha}{\hbar}V(\cdot-X')\right]}e^{\frac{it}{\varepsilon}\frac{\hbar}{2M}\partial_x^2}\,\psi, \qquad (2.17)$$

where we used the small mass ratio, namely $m = \varepsilon M$.

Roughly speaking, the role of $\Omega_+^{-1}(X')$ is to map the initial wave function of the light particle into the corresponding "scattered" state. In other words, in the small mass ratio approximation the whole interaction between the two particles occurs at time zero, and is completely described by the action of $\Omega_+(X')$. The motion of the heavy particle is then governed by the free Hamiltonian, but the initial state must be replaced by the scattered state.

A further approximation can be introduced, that consists in neglecting the width of the bumps of the initial wave function of the heavy particle. To this aim, assume that the wave packet φ_0 is concentrated around its centre, i.e. σ_H in (2.6) is small. Then, one can replace $\Omega_+(X')$ by $\Omega_+(X_0)$ in the first summand of the r.h.s. of (2.15), and by $\Omega_+(-X_0)$ in the second one. As a consequence, one can approximate $\psi_a^\varepsilon(t)$ by

$$\begin{aligned}\psi_b^\varepsilon(t,x,X) &= \frac{M\sqrt{\varepsilon}}{2\pi i\hbar t}\left[\int_{-\infty}^{+\infty} e^{i\frac{M(X-X')^2}{2\hbar t}}\varphi_0(X'-X_0)e^{-i\frac{P_H X'}{\hbar}}\,dX'\right.\\ &\qquad\qquad \times\int_{-\infty}^{+\infty} e^{i\frac{M\varepsilon(x-x')^2}{2\hbar t}}\Omega_+^{-1}(X_0)\chi_0(x')\,dx'\\ &\quad+\int_{-\infty}^{+\infty} e^{i\frac{M(X-X')^2}{2\hbar t}}\varphi_0(X'+X_0)e^{i\frac{P_H X'}{\hbar}}\,dX'\\ &\qquad\qquad \left.\times\int_{-\infty}^{+\infty} e^{i\frac{M\varepsilon(x-x')^2}{2\hbar t}}\Omega_+^{-1}(-X_0)\chi_0(x')\,dx'\right], \qquad (2.18)\end{aligned}$$

and the related error reads

$$\|\psi_a^\varepsilon(t) - \psi_b^\varepsilon(t)\|_{L^2(\mathbb{R}^2)} \leq C_T\, \alpha\, \sigma_H\, \|V'\|_2\,, \quad \forall t \in [0,T]\,, \tag{2.19}$$

as one can easily prove refining Proposition 3.2 of [3] and applying it to the present special case with initial data (2.5), (2.6) and potential (2.4).

Notice that the function $\psi_b^\varepsilon(t)$ is the sum of two factorized states, so it exhibits a remarkably simpler structure than $\psi_a^\varepsilon(t)$.

Computing now the heavy particle probability density corresponding to (2.18), yields

$$\begin{aligned}\rho_b^\varepsilon(t,X) \;:=\; &\left|(\mathcal{U}^M(t)\varphi_0)(X - X_0 + P_H t/M)\right|^2 + \left|(\mathcal{U}^M(t)\varphi_0)(X + X_0 - P_H t/M)\right|^2 \\ &+2\mathrm{Re}\left[\Lambda e^{-2i\frac{P_H}{\hbar}X}(\mathcal{U}^M(t)\varphi_0)(X - X_0 + P_H t/M)\overline{(\mathcal{U}^M(t)\varphi_0)(X + X_0 - P_H t/M)}\right]\,,\end{aligned} \tag{2.20}$$

where the decoherence coefficient Λ is given by

$$\Lambda := \int_{-\infty}^{+\infty} \overline{\Omega_+^{-1}(X_0)\chi_0(x)}\; \Omega_+^{-1}(-X_0)\chi_0(x)\, dx. \tag{2.21}$$

Remark now that formula (2.20) at time $t = \bar{t}$ is nothing but the Joos-Zeh approximation (2.13). By the definition (2.21) it appears that the decoherence coefficient Λ depends on the initial wave function χ_0 of the light particle, on the interaction potential V, and on the initial distance $2X_0$ between the centres of the two bumps of the heavy particle.

Let us observe here that the Cauchy-Schwarz inequality implies $|\Lambda| \leq 1$, so the interference fringes are diminished as compared to the non-interacting case (2.10). Indeed, for $t = \bar{t}$ the probability density (2.20) gives the profile of Figure 3.

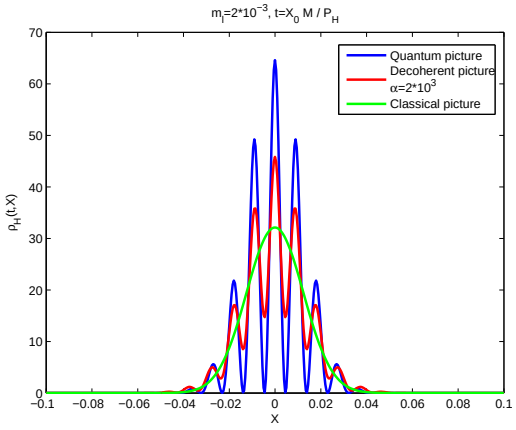

Figure 3: Partially decoherent superposition of the two heavy particle bumps.

Before entering in the details of our numerical resolution, let us stress once again the relevant difference between the evolution equations (2.3) and (2.14), i.e. the rescaling of the potential by the factor ε^{-1}. At a first glance this factor could seem quite unphysical. Nonetheless, it plays a fundamental role in the occurrence of the decoherence effect,

isolating it from other phenomena like dissipation, repulsion or deformation of the wave-packet envelope. Notice that, without introducing such a rescaling, in the limit $\varepsilon \to 0$ the scattering of the light particle would carry no effect on the heavy particle.
We stress once again that, on a qualitative level, there is no difference between this case and the case with many light particles. In the latter, decoherence would arise stronger, being dependent on the number of interactions between the heavy and the light particles. As already explained in the introduction, due to the numerical difficulties in considering several light particles, related to the dimensionality of the model, we shall focus on the two-body problem.

3 Numerical resolution

This section is concerned with the numerical resolution of the two-particle time-dependent Schrödinger problem

$$\begin{cases} \mathbf{i}\hbar\partial_t\psi = -\frac{\hbar^2}{2M}\Delta_X\psi - \frac{\hbar^2}{2m}\Delta_x\psi + \frac{\alpha}{m}V(|x-X|)\,\chi_{[0,T_{int}]}(t)\,\psi\,, \quad \text{for} \quad (x,X)\in\Omega\,,\ t\geq 0 \\ \partial_x\psi(t,x,X) = 0 \quad \text{on} \quad \partial\Omega_x\times\Omega_X\,; \qquad \partial_X\psi(t,x,X) = 0 \quad \text{on} \quad \Omega_x\times\partial\Omega_X \\ \psi(0,x,X) = \psi_0(x,X)\,, \quad \text{for} \quad (x,X)\in\Omega\,, \end{cases} \tag{3.22}$$

where $\Omega = \Omega_x \times \Omega_X$ is a bounded simulation domain with boundary $\partial\Omega = \partial\Omega_x \times \Omega_X \cup \Omega_x \times \partial\Omega_X$. The obtained numerical simulation results are presented and analyzed. In particular, the decoherence coefficient $\Lambda(\alpha)$ is computed as a function of the strength of the interaction between the particles and the resulting Joos-Zeh approximation formula is compared with the numerical solution.

Before entering into the details of our numerical method, let us comment on some relevant questions we had to face when performing the simulations.
Even though in the idealized physical experiment the two particles evolve in the whole $\mathbb{R}\times\mathbb{R}$ position space, numerically we are forced to solve the two-particle Schrödinger equation on a bounded simulation domain Ω. Thus, we are led to impose boundary conditions. In order to simplify the numerical resolution of problem (3.22), we choose homogeneous Neumann boundary conditions, the particles being thus reflected once having reached the boundary $\partial\Omega$. On the other hand, absorbing boundary conditions, which would permit the particles to get in and out of the simulation domain, would be more realistic from a physical point of view, but would considerably complicate the numerical resolution. Furthermore, in this first work we choose to focus on the decoherence effect produced by a single collision between the heavy and the light particle. This fact shall permit us to avoid the implementation of artificial (or absorbing) boundary conditions and to get precise results even when using Neumann boundary conditions. Let us comment on this, in particular on the choice of T_{int} and of the other parameters.

According to Joos and Zeh, in the regime of pure decoherence the evolution of the bumps in the heavy particle probability density is approximately free, as far as the bumps do not overlap. Thus, the evolution consists of two phenomena: first, the centres

of the bumps move with velocity $\pm P_H/M$; second, each bump spreads at a time rate proportional to M. Since we are interested in measuring the progressive disappearance of the interference fringes, the width σ_H of the initial wave packet of the heavy particle has to be chosen sufficiently large, in order to distinguish several fringes inside it, while the mass M of the heavy particle must be chosen in such a manner that there is no important diffusion within the simulation time $[0, T]$. The final time T is fixed in such a manner to permit one overlap of the heavy-particle bumps.

On the other hand, due to the small mass ratio hypothesis $m = \varepsilon M$, the light particle disperses on a time scale of order ε, thus in the time interval $[0, T]$ the light particle should be pushed outside the simulation domain. Nonetheless, due to the choice of homogeneous Neumann boundary conditions, the probability density of the light particle is reflected when touching the boundary and remains inside the simulation domain, where it keeps interacting with the heavy particle and perturbing its evolution. Clearly, this phenomenon is an artefact of our choice of boundary conditions (2.3). In order to face this problem, we notice that, due to the fast dispersion of the light particle, the collision between the two particles is completed in a time interval of duration $T_{int} \simeq \varepsilon$.

This fact can be easily proved as follows: first, we fix a threshold δ of the acceptable error. Then, we consider the following well-known identity involving the Møller operator $\Omega_+^{-1}(X_0)$ (see e.g. formula (2.24) in [2])

$$\mathcal{U}^M(-\frac{t}{\varepsilon})e^{i\frac{t}{\varepsilon}\left(-\frac{\hbar}{2M}\Delta+\frac{\alpha}{\hbar}V(\cdot-X_0)\right)}\chi_0-\Omega_+^{-1}(X_0)\chi_0 = \int_{t/\varepsilon}^{\infty}\mathcal{U}^M(-s)V(\cdot-X_0)e^{is\left(-\frac{\hbar}{2M}\Delta+\frac{\alpha}{\hbar}V(\cdot-X_0)\right)}\chi_0\,ds.$$

The previous identity shows that, if one considers the heavy particle as a fixed scatterer located at X_0, then the evolution of the light particle can be approximated by the action of the operator $\Omega_+^{-1}(X_0)$ for sufficiently large values of t/ε.
In other words, the interaction between the two particles can be considered as complete after a time T_{int} if for any $t > T_{int}$ one has

$$\left\|\int_{t/\varepsilon}^{\infty}\mathcal{U}^M(-s)V(\cdot-X_0)e^{is\left(-\frac{\hbar}{2M}\Delta+\frac{\alpha}{\hbar}V(\cdot-X_0)\right)}\chi_0\,ds\right\|_2 \;\leq\; \delta. \tag{3.23}$$

Since in (3.23) the time t always appears with the factor ε^{-1}, the interaction time T_{int} must be of order ε.

Therefore, we shall switch the interaction potential on during a short time $T_{int} \sim \varepsilon$ only, by introducing the factor $\chi_{[0,T_{int}]}(t)$ in (3.22). Thus, for $t > T_{int}$ the evolution of the probability density ρ_H associated to the heavy particle is free and hence unperturbed by the further presence of the light particle within the simulation domain. We observe, by the way, that the evolution of the light particle after the collision is of no interest for us.

It remains to discuss the role of the Neumann boundary conditions. As already stressed, they make our numerical model different from the starting problem (2.3). The choice was dictated by the fact that absorbing or transparent boundary conditions on the variable x of the light particle would make the norm of the two-particle wave function vanishes as the light particle is spreading out of the simulation domain, leading to the loss of all information concerning the heavy particle.

Besides, in order to preserve the symmetry between the two bumps we chose as initial data χ_0 of the light particle a Gaussian wave packet whose centre does not move, endowed with a width σ_L small enough to ensure that it is scattered in a sensitively different way by the two bumps of the heavy particle. As a consequence, the Fourier transform $\widehat{\chi}_0$ of χ_0 is quite spread around the origin, so unavoidably there are fast components of χ_0 that have the time to be reflected by the boundary and therefore to interact more than once with the heavy particle. On the other hand, the low frequency components of χ_0 do not meet the heavy particle at all during the time interval $[0, T_{int}]$. Therefore, the numerical experiments do not reproduce a single scattering event between the two particles, but rather a complicate interaction of duration T_{int} where the role of the boundaries is relevant. We evaluate such a role in the forthcoming paper [4], where a faster numerical scheme shall allow repeated experiments on larger domains.

Anyway, the Joss-Zeh hypothesis remains effective, for it requires the validity of the scattering regime, which is true for our numerical model too since the asymptotic evolution of the system is free.

3.1 Time-splitting method

The resolution of the Schrödinger equation (3.22) is rather delicate due to multi-scale effects. As stressed in Sections 1 and 2, we can single the decoherence effect out as far as we push the quantity $\varepsilon := m/M$ towards zero. However, for too small values of ε, problem (3.22) becomes highly anisotropic, implying severe numerical problems. Two different time scales occur, the slow time scale of the heavy particle and the fast time scale of the light one. Very fine space and time meshes are then required in order to catch the rapid evolution and guarantee good numerical approximations. These fine grids lead then necessarily to high numerical costs, making the choice of the numerical method an essential step in the resolution of (3.22).

Three different methods to solve (3.22) are compared in detail in [23] from the point of view of the numerical analysis, including issues like error estimates and convergence. It turns out that that the most advantageous method, the one we employ here, is the Peaceman-Rachford splitting method, which is second order accurate in both time and space and furthermore unconditionally stable in the L^2-norm. Let us now present this method. For more details, we refer the reader to [23].

Let $\Omega = \Omega_x \times \Omega_X = [-L, L] \times [-H, H]$ be the simulation domain, $[0, T]$ the time interval and let us discretize these spaces as follows

$$-L = x_1 \leq \cdots \leq x_i \leq \cdots x_N = L\,, \quad -H = X_1 \leq \cdots \leq X_j \leq \cdots X_M = H\,,$$

$$0 = t_1 \leq \cdots \leq t_n \leq \cdots t_K = T\,.$$

Let us moreover suppose, for simplicity, that the chosen discretizations are homogeneous, with the corresponding space/time steps $h_x > 0$, $h_X > 0$, $\Delta t > 0$. In the following, ψ_{ij}^n shall denote the approximation of $\psi(t_n, x_i, X_j)$.

Then, starting from the initial condition ψ^0, the idea is to treat the two directions separately. We advance first a half-time step $\tau = \frac{\Delta t}{2}$ and solve for each fixed $x \in \Omega_x$ the

1D stationary equation

$$\begin{cases} \frac{\hbar^2}{2M}\Delta_X\psi^{n+1/2} + \frac{\mathbf{i}\hbar}{\tau}\psi^{n+1/2} = \left(\frac{\mathbf{i}\hbar}{\tau} + \frac{\alpha}{m}V\right)\psi^n - \frac{\hbar^2}{2m}\Delta_x\psi^n\,, \quad \text{for all} \quad X \in \Omega_X\,, \\ \partial_X\psi^{n+1/2}(x,X) = 0\,, \quad \text{for all} \quad X \in \partial\Omega_X\,, \end{cases} \tag{3.24}$$

in order to get $\psi^{n+1/2}(x,\cdot)$. Afterwards, we advance a further half-time step to find $\psi^{n+1}(\cdot,X)$, for each fixed $X \in \Omega_X$, via

$$\begin{cases} \frac{\hbar^2}{2m}\Delta_x\psi^{n+1} + \left(\frac{\mathbf{i}\hbar}{\tau} - \frac{\alpha}{m}V\right)\psi^{n+1} = \frac{\mathbf{i}\hbar}{\tau}\psi^{n+1/2} - \frac{\hbar^2}{2M}\Delta_X\psi^{n+1/2}\,, \quad \text{for all} \quad x \in \Omega_x\,, \\ \partial_x\psi^{n+1}(x,X) = 0\,, \quad \text{for all} \quad x \in \partial\Omega_x\,. \end{cases} \tag{3.25}$$

One of the advantages of this procedure is that it decomposes the initial 2D Schrödinger problem (3.22) in two 1D sub-problems (3.24)-(3.25), which significantly accelerates the numerical resolution of our problem. Indeed, instead of solving (for example with a Crank-Nicolson scheme) one very large linear system (corresponding to a 2D problem), we shall solve several small linear systems via the Peaceman-Rachford scheme. This shall also permit considerable savings in memory. Moreover, another crucial advantage is that this procedure separates the two different time-scales, permitting thus different treatments for the two sub-problems.

Introducing now the following operators

$$A := -\frac{\hbar}{2M}\Delta_X\,, \quad A : D(A) \subset L^2(\Omega) \to L^2(\Omega)\,,$$

$$B := -\frac{\hbar}{2m}\Delta_x + \frac{\alpha}{m\hbar}V\,, \quad B : D(B) \subset L^2(\Omega) \to L^2(\Omega)\,, \quad G := A + B\,,$$

with $D(A)$ and $D(B)$ their definition domains, we can rewrite the semi-discrete system (3.24)-(3.25) as follows

$$\begin{cases} (I + \mathbf{i}\tau A)\psi^{n+1/2} = (I - \mathbf{i}\tau B)\psi^n\,, \\ (I + \mathbf{i}\tau B)\psi^{n+1} = (I - \mathbf{i}\tau A)\psi^{n+1/2}\,. \end{cases} \tag{3.26}$$

Discretizing now the continuous, unbounded operators A and B in space, by means of a standard second order method, leads to a set of tridiagonal linear systems to be solved in order to get the unknowns ψ_{ij}^n. Denoting by A_{NM} resp. B_{NM} the matrices approximating respectively A and B, the fully numerical scheme, called Peaceman-Rachford scheme, simply writes

$$\psi^{n+1} = (I + \mathbf{i}\tau B_{NM})^{-1}(I - \mathbf{i}\tau A_{NM})(I + \mathbf{i}\tau A_{NM})^{-1}(I - \mathbf{i}\tau B_{NM})\psi^n\,, \quad \forall n \in \mathbb{N}\,. \tag{3.27}$$

The choice of the time and space discretization steps h_x, h_X, τ is guided by the next convergence result, proved in [23].

Theorem 1 *(**Convergence**)*
The scheme (3.27) is unconditionally stable and second order accurate in time and space.

In particular the error between the exact solution ψ and the numerical solution is given by

$$||\mathcal{P}_{NM}(\psi(t_n)) - \psi^n||_2 \leq Ct_n \left[\frac{(\Delta t)^2}{\varepsilon^3} + \left((\Delta X)^2 + \frac{(\Delta x)^2}{\varepsilon} \right) ||\psi_0||_{H^4(\Omega)} \right], \qquad (3.28)$$

where $\mathcal{P}_{NM}$ is the projection of the exact solution on the space grid and $\varepsilon = m/M$. Moreover, this scheme is conserving the probability density up to a small error, which means

$$||\psi^n||_2 = ||\psi^0||_2 \left(1 + \mathcal{O}\left(\frac{(\Delta t)^2}{\varepsilon^2} \right) \right), \quad \forall n \in \mathbb{N}.$$

As one can observe from the error estimate (3.28), if we let $m \to 0$, then we are forced to chose more and more refined meshes, in particular $\Delta x \to 0$ and $\Delta t \to 0$, in order to get accurate results. This is rather restrictive from a numerical point of view and alternative methods have to be adopted. From a mathematical point of view, the 2D time-dependent Schrödinger equation is singularly perturbed for $m \to 0$. Boundary layers or multiple scale problems may occur, such that adapted methods have to be used to compute the solution in a precise manner. Work in this direction is for the moment in preparation [4].

3.2 Numerical results

In this section we present the numerical results obtained with the Peaceman-Rachford splitting method (3.27) for the resolution of (3.22). In Table 1 we summarize the parameters we used. The performed numerical experiment show that the chosen grid is sufficiently fine to capture the decoherence effect accurately, as further refinements do not change significantly the evaluation of the decoherence coefficient Λ (see Fig. 6). Moreover, we found a range of values of m and α for which the limit $\varepsilon \to 0$ is likely to be found, in the sense that, for fixed α, varying m in this range leaves Λ essentially untouched. Let us go into more details.

$L = H$	$2 * 10^{-1}$	$N = M$	401
T	$1.92 * 10^{-2}$	K	$120 * 400 + 1$
$\hbar$	1	P_H	$3.4 * M$
M	100	X_0	$5 * 10^{-2}$
m_l	$l * 10^{-3}, \quad l = 1, \cdots, 6$	P_L, x_0	0
T_{int}	$l * 48 * 10^{-7}, \quad l = 1, \cdots, 6$	$\sigma_H = \sigma_L$	10^{-2}
$\overline{t}$	$1.47 * 10^{-2}$	α	$0, \cdots, 40 * 10^2$

Table 1: Parameters used in the numerical simulations.

The different curves of Figure 4 portray the interference pattern of the probability density $\rho_H(\overline{t}, X)$ of the heavy particle at collision time $\overline{t} := X_0 M/P_H$, for $m = 2 * 10^{-3}$ and different values of the strength $\alpha \in \mathbb{R}^+$ of the potential (2.4). The decoherence effect can be clearly observed in the figures, as the interference pattern is more and more reduced.

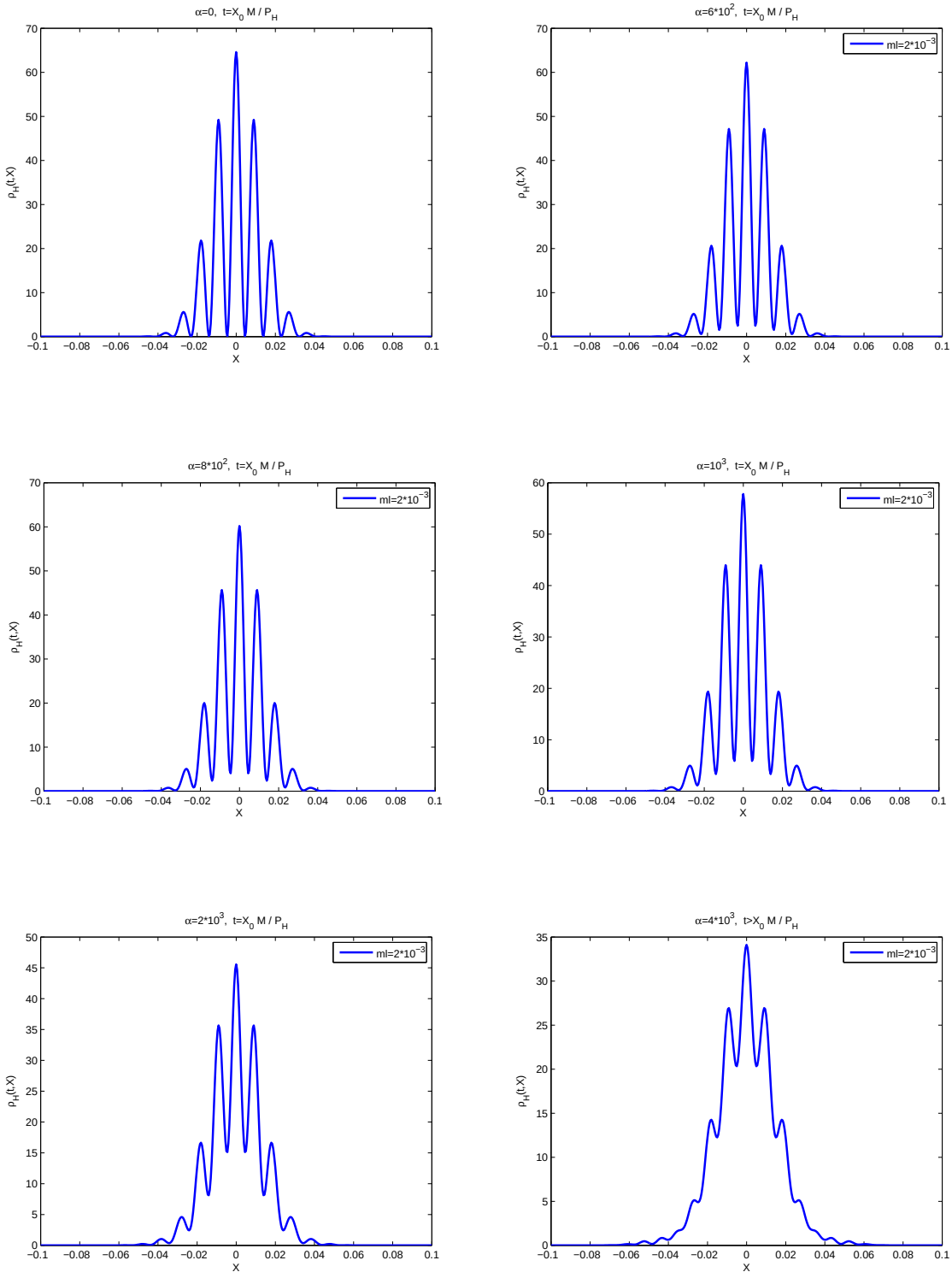

Figure 4: Decoherence effect on the heavy particle due to the interaction with the light particle. We plot the probability density of the heavy particle at $\overline{t} := X_0 M/P_H$ for different values of the strength $\alpha > 0$ of the interaction. In correspondence to the largest tested value of α, i.e. $\alpha = 4000$, the maximal overlap between the two bumps is attained at a time significantly larger than $\bar{t}$. This means that for such a strong interaction the Joos-Zeh approximation fails.

In Figure 5 (on the left), we plotted the decoherence coefficient $\Lambda(\alpha)$ as a function of the interaction strength for three different masses m. The values of $\Lambda(\alpha)$ are obtained as follows: first, we solved the Schrödinger equation (3.22) up to time $t = \overline{t}$ and evaluated $\psi_{num}(\overline{t}, x, X)$. Then, we computed $\rho_{H,num}(\overline{t}, X)$, integrating over the light particle variable x. At this stage, as we are in the small mass ratio regime $0 < m/M \ll 1$, we assume that $\rho_{H,num}$ can be approximated by the Joos-Zeh formula (2.13) and evaluating at $X = 0$ we compute

$$\Lambda(\alpha) = \frac{\rho_{H,num}(\overline{t}, X = 0)}{2\left|\left[\mathcal{U}^M(\overline{t})\varphi_0\right](X = 0)\right|^2} - 1\,.$$

Now, inserting the quantity $\Lambda(\alpha)$ in the Joos-Zeh approximation (2.13), we compare in Figure 5 (on the right) $\rho_{H,num}(\overline{t}, X)$ and $\rho_{H,JZ}(\overline{t}, X)$ over the whole domain Ω_X.
We plotted the curve $\Lambda(\alpha)$ for three different value of the mass m -i.e. for three different values of ε- in order to verify whether the asymptotic regime $\varepsilon \to 0$ had been singled out. If so, then the decoherence would remain the same as the mass becomes smaller and smaller. This is indeed the case for $m = 2 * 10^{-3}$ and $m = 3 * 10^{-3}$, but the curve corresponding to $m = 10^{-3}$ is rather different. The reason for this disagreement is made clearer by Figure 6, where we plotted the L^2-relative error between $\rho_H(\bar{t}, \cdot)$ and a reference solution $\rho_{H,ref}(\bar{t}, \cdot)$ obtained by an implementation on a much finer space-time grid. What can be observed is that for the chosen grid of $N = M = 401$ space points and $K = 120 * 400 + 1$ the test cases with $m_l = 10^{-3}$ are not precise. In fact, as $\varepsilon \to 0$, one has to choose finer and finer grids in order to keep the same accuracy, as we have to cope with a highly anisotropic or multi-scale problem. As a consequence, the plots presented in Figure 4 correspond to $m_l = 2 * 10^{-3}$.

One can also observe that. as α increases, the three curves become more distant from one another. In order to explain this phenomenon, we recall that in the approximation ψ_b^ε introduced in (2.18) there is a source of error which is increasing in α and independent of ε, as estimate (2.19) shows. This means that for large values of α we cannot expect to remain in the asymptotic regime, nor even that such a regime exists.
In order to investigate the actual existence of such a regime one should push ε further towards zero, but then numerical errors would arise and possibly take the overhand, as detailed above. As a consequence, we can argue that this source of numerical error plays a role also in the straight curve in Figure 5 for α around 3000. In this range of values of the interaction such error adds to the Joos-Zeh approximation error.

Besides, it is worth remarking that for $\alpha \geq 3000$ the maximal overlap of the two bumps in the probability density of the heavy particle is not verified for $t = \bar{t}$, but later. Furthermore, the time of maximal overlap increases with the strength α of the interaction, even though the overall profile of the probability density remains close to the one of a purely decoherent state. This phenomenon can be explained as follows: first, as already noticed, if the interaction is not too strong, then the Joos-Zeh approximation is effective and thus the only effect of the interaction on the heavy particle is the occurrence of decoherence. Second, if the strength of the interaction overcomes a certain threshold, then the Joos-Zeh approximation is no longer valid, but the shape of the probability

density is not lost: what happens is that the two heavy bumps are slowed down, so that it results that the main effect beyond decoherence is the repulsion between the bumps. This is not a trivial point, as repulsion could be expected to emerge together (or later than) the destruction of the shape of the probability density.

We then conclude that we verified the validity of an approximation of the type Joos-Zeh for the model (3.22) in the regime $\alpha \leq 10$, $m \leq 3 \cdot 10^{-3}$, neglecting the numerical errors which arise for $m \leq 10^{-3}$.

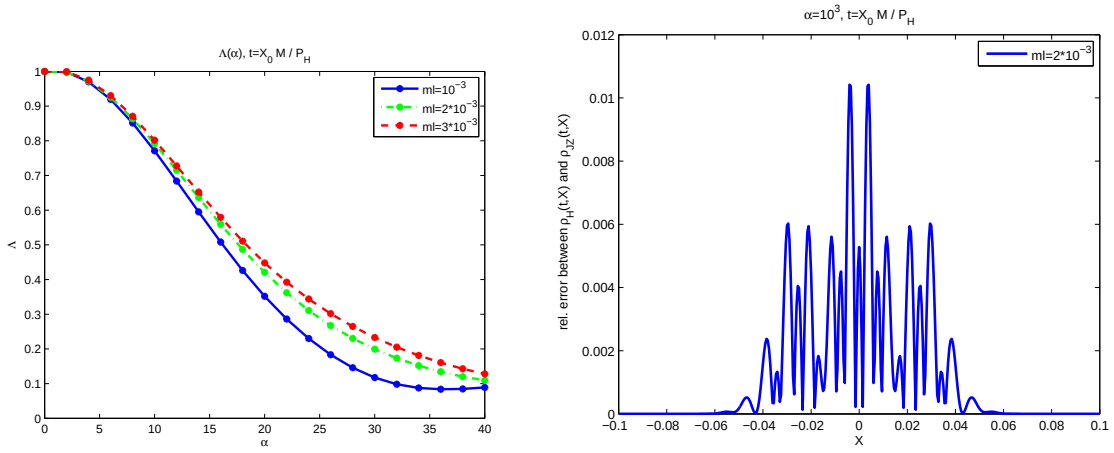

Figure 5: Left: The decoherence coefficient $\Lambda(\alpha)$. Right: The relative error between the numerical solution $\rho_H(\bar{t}, X)$ and the Joos-Zeh approximation $\rho_{JZ}(\bar{t}, X)$.

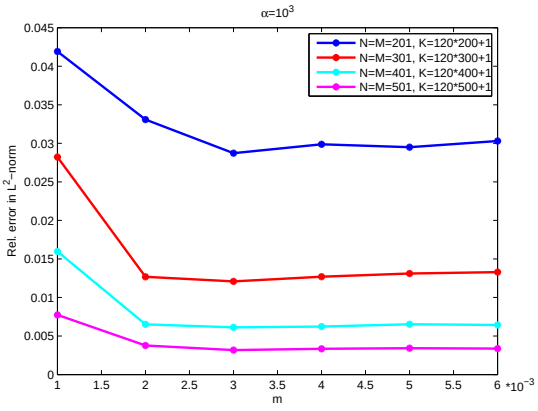

Figure 6: L^2-relative error $||\rho_H(\bar{t}, \cdot) - \rho_{H,ref}(\bar{t}, \cdot)||_2 / ||\rho_{H,ref}(\bar{t}, \cdot)||_2$, where $\rho_{H,ref}(\bar{t}, \cdot)$ is a reference solution computed on a refined grid.

4 Understanding decoherence in the configuration space of the two-particle system

In order to analyze the occurrence of decoherence, in the previous sections we followed the traditional approach that consists in computing the decrease of the non-diagonal terms of the density matrix of the heavy particle. As shown in Section 2.3, this is equivalent to describing the disappearance of the interference fringes. In other words, we focused on the open system "heavy particle".

On the other hand, decoherence can be discerned also by following the evolution of the two-body wave function $\psi(t, x, X)$, namely, analyzing the dynamics of the closed system given by the heavy and the light particle together. Quite surprisingly, in such a framework the occurrence of decoherence has a clear origin and an effective pictorial representation.

The two plots in Figure 7 portray the real part and the square of the modulus of the two-particle initial data ψ_0. Notice that the probability density concentrates in two bumps near the points $x = 0$, $X = \pm X_0$. Notice also that as the light particle has no velocity, no oscillations occur in the x-direction on the left figure.

Let us first consider the non-interacting (free) evolution (i.e. $V \equiv 0$). The two heavy bumps start moving towards each other along the vertical direction. Obviously, such a dynamics preserves the "left-right symmetry" $\psi(t, x, X) = \psi(t, -x, X)$ inherited by the initial wave function, as shown in the two lower plots of Figures 8 and 9. As a consequence, at time $\bar{t} = MX_0/P_H$, the overlap between the two components of the wave function is perfect, so that the effect of the composition of the phases becomes maximal: in particular, the peaks of the modulus squared of the wave function are emphasized and there are regions where the same modulus squared is zero (namely, the dark regions in the fourth picture in Figure 9).

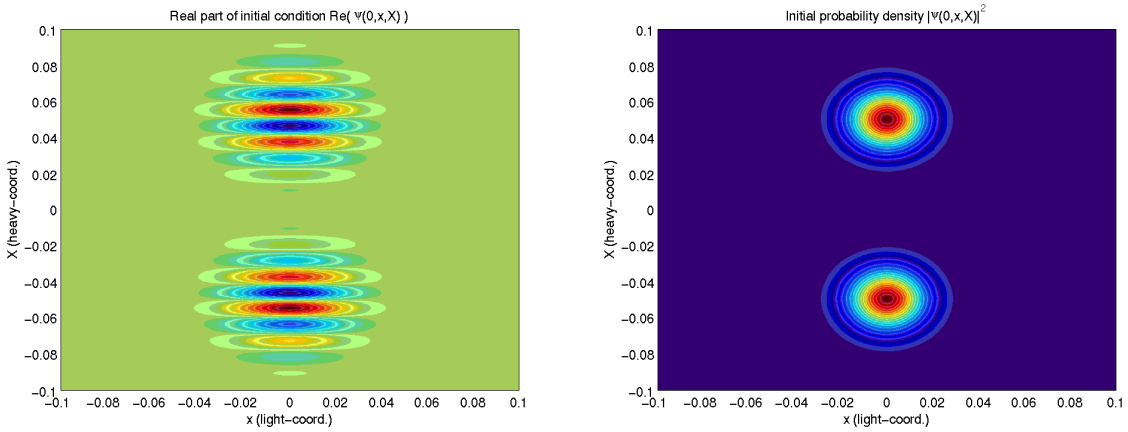

Figure 7: Left: 2D Plot of the real part of the initial condition $\psi_0(x, X) = \chi(x)\varphi(X)$ (uncorrelated). Right: Squared absolute value of the same initial condition.

Let us now consider the interacting case. The upper part of Figures 8 and 9 shows that the left-right symmetry is broken. Such an effect is put in best evidence in Figure

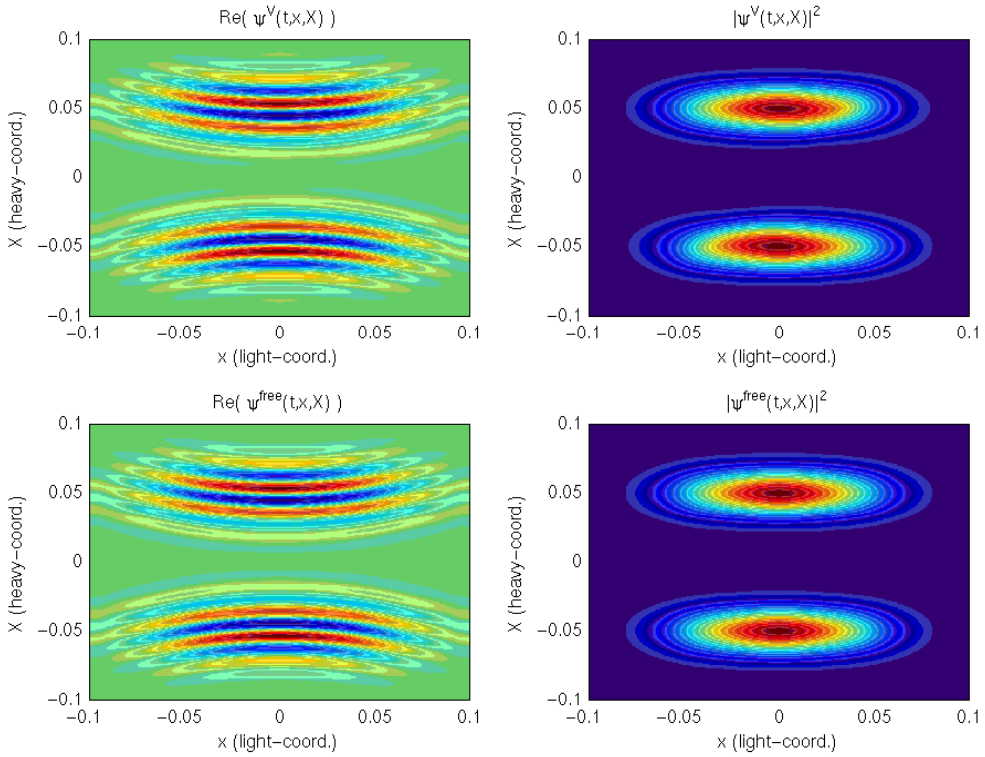

Figure 8: Left: 2D Plot of the real part of the 2-body interacting wave fct. $\psi^V(t,x,X)$ resp. non-interact. $\psi^{\text{free}}(t,x,X)$ at time $t \in [0, T_{int}]$. Right: Squared absolute value of the same wave fct.

10, where the difference between the real part of the wave function in the interacting case and in the non-interacting case is plotted. Notice in particular that, due to the repulsive character of the interaction, the "upper" bump is moved towards the right region of the picture, while the "lower" bump is shifted to the left. The same comments apply to Figure 11.

As a consequence, at time $\bar{t}$ the two bumps cannot overlap perfectly, therefore the composition of the phases of the two bumps is not so effective and, as a result, the interference is attenuated. In particular, a comparison between the second and the fourth picture in Figure 9 shows that the maxima of the modulus squared of the wave function are lower and the dark regions are less extended than in the non-interacting case. In other words, decoherence has occurred.

In order to better underline the relationship between this insight of decoherence and the attenuation of the interference computed in Section 3, we recall that the plots in Figure 4 correspond to a one-particle representation, that is obtained integrating the two-particle probability density over the light-particle variable x. Therefore, the plots in Figure 4 can be interpreted as follows: if one considers the heavy particle variable X only, then the two bumps seem to overlap completely. In fact, the presence of the light particle introduces another degree of freedom, represented by the variable x. If the two particles interact with each other, then the two bumps becomes far apart along such variable x, so their overlap is only apparent. We remark that this description of the

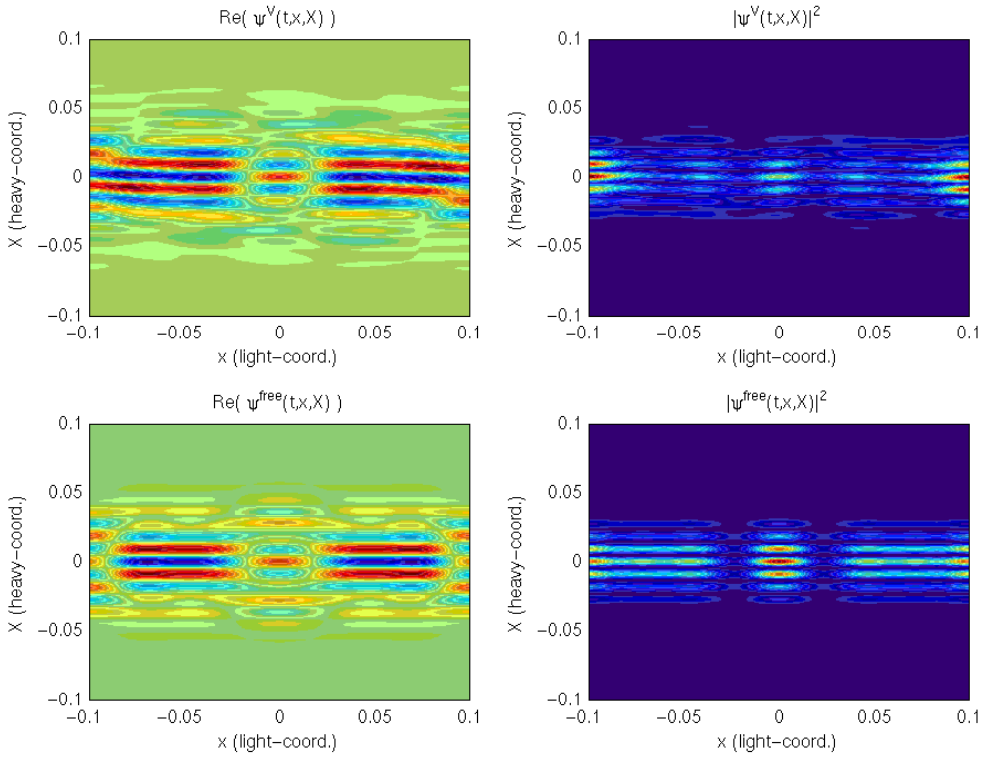

Figure 9: Same plots at the complete overlap time $\overline{t} = \frac{X_0 M}{P_H}$

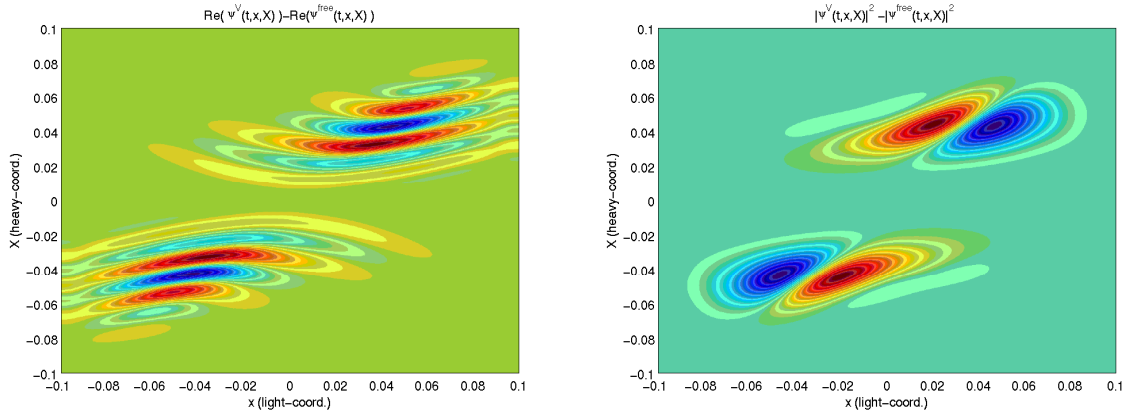

Figure 10: Dephasing effect. Left: Plot of the difference $\mathcal{R}e(\psi(t,x,X)) - \mathcal{R}e(\psi^{\text{free}}(t,x,X))$ for $t \in [0, T_{int}]$. Right: Plot of the difference $|\psi(t,x,X)|^2 - |\psi^{\text{free}}(t,x,X)|^2$ for $t \in [0, T_{int}]$.

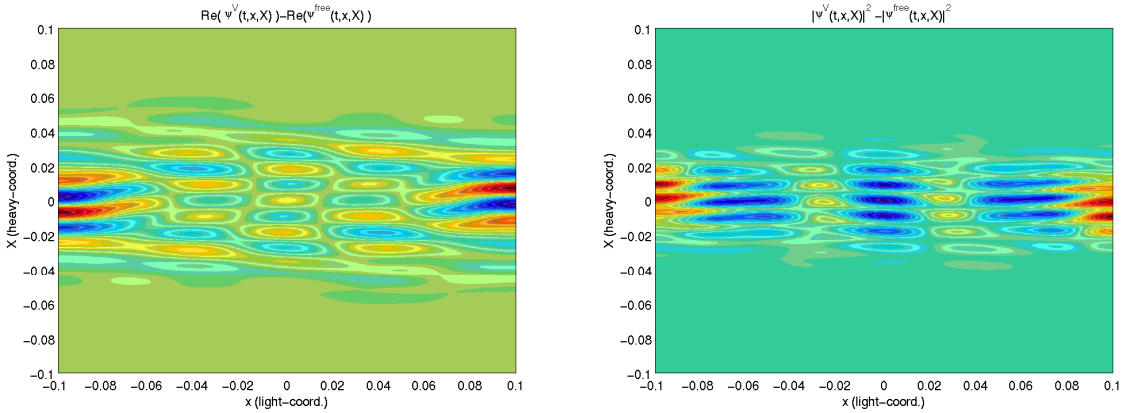

Figure 11: Dephasing effect. Left: Plot of the difference $\mathcal{R}e(\psi(t,x,X)) - \mathcal{R}e(\psi^{\text{free}}(t,x,X))$ for $t = \overline{t}$. Right: Plot of the difference $|\psi(t,x,X)|^2 - |\psi^{\text{free}}(t,x,X)|^2$ for $t = \overline{t}$.

phenomenon of decoherence coincides with the mechanism singled out in the context of the Bohmian interpretation of quantum mechanics [13], [16].

5 Conclusion

We presented in this paper the results of numerical simulations that show the decoherence effect induced on a heavy particle by the repulsive interaction with a light one. To this aim, the 2D time-dependent Schrödinger equation has been solved via a time-splitting scheme. The obtained results are helpful to complete the analytical study, presented in previous works [2, 3]. In particular, through the numerical exploration a suitable range is found, where the approximations used in the cited papers holds true. A more realistic model, describing multiple collisions, shall be the objective of a future work.

Acknowledgments. This work has been supported by the GREFI-MEFI (Groupement De Recherche Européen Franco-Italien) and the ANR QUATRAIN (Quantum transport in nanostructures). The authors would like to thank the Laboratoire LATP of the University of Provence and the University of Milano Bicocca for the support and the kind hospitality.

References

[1] R. Adami, L. Erdős, *Rate of decoherence for an electron weakly coupled to a phonon gas*, J. Stat. Phys. **132** (2008), no. 2, 301–328.

[2] R. Adami, R. Figari, D. Finco, A. Teta, *On the asymptotic behaviour of a quantum two-body system in the small mass ratio limit*, J. Phys. A: Math. Gen., **37** (2004), 7567–7580.

[3] R. Adami, R. Figari, D. Finco, A. Teta, *On the asymptotic dynamics of a quantum system composed by heavy and light particles*, Comm. Math. Phys. **268** (2006), no. 3, 819–852.

[4] R. Adami, M. Hauray, C. Negulescu *Accelerate and precise numerical resolution of the anisotropic two-body Schrödinger equation. Application to decoherence*, in preparation.

[5] A. Bertoni, *Simulation of Electron Decoherence Induced by Carrier-Carrier Scattering*, J. Comp. El. **2** (2003), 291–295.

[6] Ph. Blanchard, D. Giulini, E. Joos, C. Kiefer, J. Kupsch, I.-O. Stamatescu, H.D. Zeh, *Decoherence and the Appearance of a Classical World in Quantum Theory*, Springer, 1996.

[7] H.-P. Breuer, F. Petruccione, *The Theory of Open Quantum Systems*, Oxford University Press, Oxford, 2007.

[8] C. Cacciapuoti, R. Carlone, R. Figari, *Decoherence induced by scattering: a three dimensional model*. J. Phys. A: Math. Gen., **38** (2005), no. 22, 4933–4946.

[9] A.O. Caldeira, A.J. Leggett, *Influence of damping on quantum interference: an exactly soluble model*, Phys. Rev. A **31** (1985), 1059.

[10] J. Clark, *The reduced effect of a single scattering with a low-mass particle via a point interaction*, J. Func. An. **256** (2009), no. 9, 2894–2916.

[11] C. Cohen-Tannoudji, B. Diu, F. Laloë *Mécanique quantique I*, Hermann éditeurs des sciences et des arts, Paris, 1998.

[12] G. Dell'Antonio, *Towards a theory of decoherence*, *Int. J. Mod. Phys. B*, **18** (2004), no. 4-5, 643–654.

[13] D. Dürr, *Bohmsche Mechanik als Grundlage der Quantenmechanik*, Springer Verlag, 2001.

[14] D. Dürr, R. Figari, A. Teta, *Decoherence in a two-particle model*, J. Math. Phys. **45** (2004), no. 4, 1291–1309.

[15] D. Dürr, H. Spohn, *Decoherence Through Coupling to the Radiation Field*, in *Decoherence: Theoretical, Experimental and Conceptual Problems*, Blanchard Ph., Giulini D., Joos E., Kiefer C., Stamatescu I.-O. eds., Lect. Notes in Phys. 538 (2000), Springer, 77–86.

[16] D. Dürr, S. Teufel, *Bohmian Mechanics. The Physics and Mathematics of Quantum Theory*, Springer, 2009.

[17] G. B. Folland, *Harmonic analysis in phase space*, Princeton University Press, 1989.

[18] G. Hagedorn, *A time dependent Born-Oppenheimer approximation*, Comm. Math. Phys. **77** (1980), no. 1, 1–19.

[19] K. Hornberger, J.E. Sipe, *Collisional decoherence reexamined*, Phys. Rev. A **68** (2003), 012105, 1–16.

[20] K. Hornberger, S. Uttenhaler, B. Brezger, L. Hackermüller, M. Arndt, A. Zeilinger, *Collisional decoherence observed in matter wave interpherometry*, Phys. Rev. Lett., **90** (2003), 160401.

[21] K. Hornberger, B. Vacchini, *Monitoring derivation of the quantum linear Boltzmann equation*, Phys. Rev. A, **77**, (2008), 022112 1–18.

[22] E. Joos, H.D. Zeh, *The emergence of classical properties through interaction with the environment*, Z. Phys., **B59** (1985), 223–243.

[23] C. Negulescu, *Numerical error analysis of a splitting method for the resolution of the anisotropic Schrödinger equation*, in preparation.

[24] R. Omnès, *The Interpretation of Quantum Mechanics* Princeton University Press, Princeton, 1994.

[25] A. Pazy *Semigroups of linear operators and applications to partial differential equations*, Springer Verlag, New-York, 1983.

[26] M. Reed, B. Simon *Methods of modern matematical physics, vol. III - Scattering theory*, Academic Press, New York, 1979.

[27] P. W. Shor *Scheme for reducing decoherence in quantum computer memory*, Phys. Rev. A **52** (1995), no. 4, 2493–2496.

[28] C. A. Stafford, D. M. Cardamone, S. Mazumadar *The quantum interference effect transistor*, Nanotechnology **18** (2007), no. 42, 1–6.

[29] W. Zhang, N. Konstantinidis, K. A. Al-Hassanieh, V. V. Dobrovitski *Modelling decoherence in quantum spin systems*, J. Phys. Condens. Matter **19** (2007), no. 8, 1–28.